

Numerical Investigation of Quenching for a Nonlinear Diffusion Equation with a Singular Neumann Boundary Condition

C. I. Christov and K. Deng

*Department of Mathematics, University of Louisiana at Lafayette,
Lafayette, LA 70504-1010*

Abstract

For a nonlinear diffusion equation with a singular Neumann boundary condition, we devise a difference scheme which represents faithfully the properties of the original continuous boundary value problem. We use non-uniform mesh in order to adequately represent the spatial behaviour of the quenching solution near the boundary.

1 Introduction

Studying nonlinear problems in thermal conductivity is of prime interest in many areas of physics. Nonlinearity can arise in the heat-conduction equation itself and/or in the boundary conditions. The former is the case when there exist internal sources of heat in the region under consideration. The latter encompasses the situations when there is radiation from the surface into an effective continuous medium. Then the boundary condition for the temperature u reads (see, e.g., [6]):

$$\kappa \frac{\partial u}{\partial n} = \sigma(u^4 - u_0^4),$$

which leads to a blow up on the boundary due to the fact that the power of u is greater than unity. A reversed situation is encountered in thermconvective boundary layers when the temperature gradient can become at certain moment of time unfavorable for the local convective motion. Since the eddy coefficient of heat diffusion κ and resistance coefficient σ are functionals of the temperature distribution then locally the following condition

$$\frac{\partial u}{\partial n} = Cu^\alpha - F(u_0), \tag{1.1}$$

can provide the most pertinent physical model for the effective thermal interaction of the convected medium and the boundaries. Note that the coefficient of laminar heat diffusion is neglected which is a reasonable approximation during the periods with dominant eddy

diffusivity. For $\alpha < 0$ a process of quenching of the temperature can be incited. Naturally the coefficient of eddy diffusion will decrease with the decrease of the temperature and ultimately one is to consider the coefficient of laminar diffusion. Yet, there is a significantly long period of time during which eq.(1.1) gives the first-order effect. A typical physical situation is the formation of inverse layers within the atmospheric boundary layer which can hinder the natural ability of the atmosphere to diffuse smog particles. For a discussion on this topic, see [1].

Recently, modeling the unsteady thermoconvective flows in vertical slots has attracted the attention due to applications to flows under reduced gravity with significant influence of the modulation part of the gravity acceleration. This is the so-called G -jitter flow (see, e.g., [2] and the literature cited therein. Due to the unsteady loading forces there take place periods of time during which the temperature gradient at the wall is unfavorable and a process of quenching can onset. The blow-up scenario is also of interest but it requires different numerical technique and will be treated elsewhere.

The objective of the present work is twofold. First, to investigate the theoretical conditions under which a quenching takes place. Second, to gather some insight about the behavior of the solution for the temperature before embarking on a full-fledged numerical simulation of G -jitter with nonlinear Neumann boundary condition. This is the applied aspect of the motivation of the present work.

2 Posing the Problem

The problem under consideration is as follows:

$$\gamma u^{\gamma-1} u_t = u_{xx} \quad 0 < x < 1, \quad 0 < t < T, \quad (2.1)$$

$$u_x(1, t) = 0, \quad u_x(0, t) = u^{-\beta}(0, t) \quad 0 < t < T, \quad (2.2)$$

$$u(x, 0) = u_0(x) \quad 0 \leq x \leq 1, \quad (2.3)$$

where $\gamma > 0$ and $\beta > 0$ are real numbers. As is well known, if $0 < \gamma < 1$, (2.1) is the porous medium equation; if $\gamma > 1$, (2.1) is a plasma type equation; if $\gamma = 1$, it reduces to the ubiquitous heat equation. Such a problem was originally studied in [5] for the limiting case of linear heat-conduction equation $\gamma = 1$. In [3] the quenching behaviour of the solution was examined, that is, the solution reaches zero in a finite time (note that the solution must be positive). To motivate our discussion in the present paper we recall two main results from [3]:

Theorem A (Finite Quenching) *Every solution of (2.1)–(2.3) quenches in a finite time under the following assumptions on the initial data:*

$$u_0(x) \geq 0, \quad u_0'(x) \geq 0, \quad u_0''(x) \leq 0, \quad (2.4)$$

and the “compatibility conditions”

$$u_0'(1) = 0, \quad u_0'(0) = u_0^{-\beta}(0). \quad (2.5)$$

Moreover, the quenching occurs only on the boundary, i.e. at $x = 0$.

Theorem B (Quenching Rate) *Suppose that*

$$u_0'(x) \geq 0 \quad \text{and} \quad u_0''(x) \leq 0.$$

Then the solution of (2.1)–(2.3) satisfies

$$C_1 \leq u(0, t)(T - t)^{\frac{1}{\gamma+2\beta+1}} \leq C_2, \quad (2.6)$$

where C_1 and C_2 are positive numbers, and T is the quenching time.

It is worth mentioning that for $\gamma = 1$, these results had been established in [4]. However, from technical point of view, the results of [4] are somewhat different from those in [3]. On the one hand, in Theorem A of [4], no assumptions are imposed on the initial data, except the compatibility conditions. On the other hand, in Theorem B of [4], more restrictive conditions are assumed.

From the above observations, a natural question arises: Without assumptions on u_0 , can Theorems A and B of [3] still hold? To our knowledge, no analytical arguments may be employed to answer the question at this stage. Therefore, in the present paper we devise a difference scheme. The guiding principle when constructing the scheme was that it faithfully represents the balance for the energy the same way as the original continuous equation does.

To verify the result of Theorem A we consider four different initial conditions. Some of them satisfy the conditions of the theorem, while the other do not.

- (i) An initial condition that satisfies behavioral conditions (2.4) and the compatibility conditions (2.5) reads

$$u_0(x) = a \cos(1 - x), \quad a = [\sin(1) \cos^\beta(1)]^{-\frac{1}{\beta+1}}, \quad x \in [0, 1]. \quad (2.7)$$

- (ii) An initial condition that satisfies the compatibility conditions and first two of the behavioral conditions is the following

$$u_0(x) = -4x^3 + 3x^2 + 6x + 6^{-\frac{1}{\beta}}, \quad x \in [0, 1]. \quad (2.8)$$

- (iii) An initial condition that satisfies the compatibility conditions and only the first of the behavioral conditions is given by

$$u_0(x) = \cos(6) - \cos(6(1 - x)) + (-6 \sin(6))^{-\frac{1}{\beta}}, \quad x \in [0, 1]. \quad (2.9)$$

- (iv) An initial condition satisfying the behavioral condition (2.4) but not satisfying the nonlinear compatibility condition is simply a constant. For definiteness we choose

$$u_0(x) = 1.483, \quad x \in [0, 1] \quad (2.10)$$

3 Difference Scheme

3.1 Non-uniform Grid and Spatial Discretization

During the quenching near the point $x = 0$ the gradients of the solution become very large. It is easy to show that the behaviour of the solution near the point $x = 0$ at the moment of quenching obeys the rule

$$u \sim [(1 + \beta)x]^{\frac{1}{1+\beta}} \quad (3.1)$$

because in that moment one has $u = 0$. This kind of local behaviour of the solution requires a non-uniform grid because of the steep increase of the sought function u . In fact, most of the time a uniform grid would be sufficient since $u(0, t) \neq 0$. Yet, in order to capture the quenching moment with high accuracy one needs a grid which is adequately dense even for the last moment of calculations, namely for $t = T_c$, where T_c is the quenching time.

There is no real need for time dependent grid whose spacings change dynamically during the evolution. It could eventually save a couple of grid points on the initial stages when u is non-singular at $x = 0$, but the re-calculating the functional values at each time step will require costly interpolation procedures and will inevitably introduce additional truncation error which will prevent us of devising a scheme with exact difference satisfaction of the energy balance.

To this end we introduce the following coordinate transformation

$$\xi = [(1 + \beta)x]^{\frac{1}{1+\beta}}, \quad \frac{d\xi}{dx} \sim [(1 + \beta)x]^{-\frac{\beta}{1+\beta}} \longrightarrow \frac{dx}{d\xi} \sim [(1 + \beta)x]^{\frac{\beta}{1+\beta}}.$$

which secures that

$$\frac{du}{d\xi} = \frac{du}{dx} \frac{dx}{d\xi} \sim [(1 + \beta)x]^{-\frac{\beta}{1+\beta}} [(1 + \beta)x]^{\frac{\beta}{1+\beta}} \sim O(1).$$

Thus the pointwise change of the solution u as function of the independent variable ξ will be approximately uniform near the quenching point $x = 0$. The latter means that the approximation will be uniform.

The above consideration allows us to set for our problem a non-uniform grid which does not depend on time. In the cases when the quenching point is not known in advance the non-uniform grid (or – which is the same – the coordinate transformation) has to be defined *a-posteriori*, i.e., it has to change during the time-stepping of the solution.

In terms of the independent variable ξ we use a staggered uniform grid

$$\xi_i = 1 - h_0(i - 1.5), \quad i = 1, 2, \dots, M, \quad h_0 = \frac{1}{M - 2}.$$

In the original domain (coordinate x) the grid points are prescribed by the following difference function

$$x_i = [h_0(i - 1.5)]^{\left(\frac{1}{1+\beta}\right)}, \quad i = 2, \dots, M - 1, \quad x_1 = -x_2, \quad x_M = 2 - x_{M-1}, \quad (3.2)$$

which means that the boundary $x = 0$ is situated exactly in the middle between the first and second grid points, while the boundary $x = 1$ is in the middle between the last two points. This is important for the second-order approximation of boundary conditions which involve derivatives. For the non-uniform x -spacing h_i we get the the following expression

$$h_{i+1} = x_{i+1} - x_i, \quad i = 1, \dots, M - 1.$$

On the non-uniform grid the difference approximation for the second spatial derivative reads

$$\Lambda u_i \stackrel{\text{def}}{=} 2 \left[\frac{h_i u_{i+1} - (h_i + h_{i+1}) u_i + h_{i+1} u_{i-1}}{h_i h_{i+1} (h_i + h_{i+1})} \right] = u''(x_i) + O(h_i h_{i+1}). \quad (3.3)$$

3.2 Temporal Discretization

Denote by τ the time increment. The superscript n on the time variable t stands for the current (“old”) time stage, and $n + 1$ for the “new” one. The following scheme akin to Crank-Nicholson scheme is used

$$\frac{2}{\gamma + 1} \left[\frac{(u_i^{n+1})^{\gamma+1} - (u_i^n)^{\gamma+1}}{(u_i^{n+1})^2 - (u_i^n)^2} \right] \frac{u_i^{n+1} - u_i^n}{\tau} = \frac{1}{2} \Lambda [u_i^{n+1} + u_i^n], \quad (3.4)$$

where Λ is the difference operator defined in (3.3).

The scheme (3.4) is nonlinear and cannot be implemented without linearization. The simplest way to do this is to introduce iterations as follows

$$\frac{2}{\gamma + 1} \left[\frac{(u_i^{n+1,k})^{\gamma+1} - (u_i^n)^{\gamma+1}}{(u_i^{n+1,k})^2 - (u_i^n)^2} \right] \frac{u_i^{n+1,k+1} - u_i^n}{\tau} = \frac{1}{2} \Lambda [u_i^{n+1,k+1} + u_i^n], \quad (3.5)$$

and to repeat them until convergence is reached in the sense that

$$\frac{\max_i \|u_i^{n+1,k+1} - u_i^{n+1,k}\|}{\max_i \|u_i^{n+1,k+1}\|} \leq \varepsilon \approx 10^{-12}.$$

The decision to use iterations enables us to use a simplest linearization of the boundary condition at $x = 0$ which reads

$$u_2^{n+1,k+1} - u_1^{n+1,k+1} = h_2 \left(\frac{u_2^{n+1,k} + u_1^{n+1,k}}{2} \right)^{-\beta}.$$

Thus at each iteration for the unknown function $u_i^{n+1,k+1}$ we are solving boundary value problem which contains only its derivatives at the boundary points. Yet, the overall problem is correct due to the term stemming from the time derivative.

3.3 Organization of the Algorithm

As initial condition for the internal iterations we use the value of the function on the previous (“old”) time step n . After the iterations converge we get the function on the “new” time stage $n + 1$. Then we move to the next time step, etc.

Special care is taken to refine the time increment τ when the solution approaches the moment of quenching. A step is executed with the current value of τ . If a negative value for $u(0, t)$ is encountered then the time increment is reduced in half and the step is repeated until a positive value is the outcome of the calculations. If a positive value is not found for $\tau < 10^{-15}$ then the process is terminated.

The refining of the time increment can be also used in order to secure good approximation near the moment of quenching when the time derivative is rather large. We choose to decrease (increase) τ in a manner that the relative increase of $u(0, t)$ is a prescribed quantity. For different values of the governing parameters this quantity can vary, say from 10^{-6} to 10^{-2} .

4 Difference Representation of the Energy Balance

In this section we consider the nonlinear implicit difference scheme which ensues from the above algorithm after the internal iterations converge. We show that it represents faithfully the energy balance as the continuous problem does.

The scalar product is introduced as follows:

$$(\phi, \psi) = \sum_{i=2}^{M-1} \frac{h_i + h_{i+1}}{2} \phi_i \psi_i.$$

Then

$$\begin{aligned} (u, \Lambda u) &= \sum_{i=2}^{M-1} u_i \left[\frac{h_i u_{i+1} - (h_i + h_{i+1}) u_i + h_{i+1} u_{i-1}}{h_i h_{i+1}} \right] \\ &= \sum_{i=2}^{M-1} \left[u_i \left(\frac{u_{i+1} - u_i}{h_{i+1}} \right) + u_i \left(\frac{-u_i + u_{i-1}}{h_i} \right) \right] \\ &= -\frac{1}{2} \sum_{i=2}^{M-1} \left[\frac{u_i^2 + u_{i+1}^2 - 2u_i u_{i+1}}{h_{i+1}} \right] - \frac{1}{2} \sum_{i=2}^{M-1} \left[\frac{u_i^2 + u_{i-1}^2 - 2u_i u_{i-1}}{h_i} \right] \\ &\quad + \frac{1}{2} \left(-\frac{u_{M-1}^2}{h_M} + \frac{u_M^2}{h_M} + \frac{u_1^2}{h_2} - \frac{u_2^2}{h_2} \right) \end{aligned}$$

The boundary conditions (2.2) are approximated as follows (the quasi-linearization will be addressed later in the text):

$$u_M = u_{M-1}, \quad u_2 - u_1 = h_2 \left(\frac{u_1 + u_2}{2} \right)^{-\beta}. \quad (4.1)$$

Then for the above scalar product we get

$$(u, \Lambda u) = -\frac{1}{2} \sum_{i=2}^{M-1} \left[h_{i+1} \left(\frac{u_i - u_{i+1}}{h_{i+1}} \right)^2 + h_i \left(\frac{u_i - u_{i-1}}{h_i} \right)^2 \right] - \left(\frac{u_1 + u_2}{2} \right)^{1-\beta}. \quad (4.2)$$

The term containing the time derivative is nonlinear which makes the scheme (3.4) to faithfully represent the properties of the original initial-boundary value problem, e.g. energy integral. To prove that we multiply both sides of (3.4) by $\frac{1}{2}[u_i^{n+1} + u_i^n](h_i + h_{i+1})$ and take the sum from $i = 2$ to $i = M - 1$. Thus we get

$$\begin{aligned} \frac{2}{\tau(\gamma + 1)} \left[\sum_{i=2}^{M-1} (u_i^{n+1})^{\gamma+1} \frac{h_i + h_{i+1}}{2} - \sum_{i=2}^{M-1} (u_i^n)^{\gamma+1} \frac{h_i + h_{i+1}}{2} \right] \\ = ([u^{n+1} + u^n], \Lambda[u^{n+1} + u^n]), \end{aligned} \quad (4.3)$$

which is an equivalent of the respective property of the differential boundary value problem. In other words, the energy-like sum (“integral”) evolves due to the (un)balance of the dissipation and energy production at the boundary with the nonlinear boundary condition. In this sense, our scheme does not contribute artificial (scheme) properties.

5 Results and Discussion

The problem under consideration depends on two governing parameters β and γ . Qualitative differences in the behaviour of the solution can be expected only when β and γ change from values smaller than unity to greater than (or equal to) unity. For instance, smaller values of β correspond to a solution with weaker singularity at $x = 0$ according to the asymptotic behavior of the local solution (3.1). Larger γ require smaller time increments τ .

We consider the following four sets of values for the governing parameters:

- $\beta = 0.5 < 1$ and $\gamma = 0.5 < 1$
- $\beta = 0.5 < 1$ and $\gamma = 2 > 1$
- $\beta = 2 > 1$ and $\gamma = 2 > 1$
- $\beta = 2 > 1$ and $\gamma = 0.5 < 1$

5.1 Initial Conditions and Quenching (Theorem A)

First we begin with the case (2.7) when the initial condition satisfies all the conditions of Theorem A. For all four sets of values for the governing parameters we encountered quenching in our numerical calculations. The spatial profile of the solution in the moment of quenching is presented in the Figure 1 for two different resolutions $N = 200$ and $N = 100$ and compared to the analytical expression for the local solution.

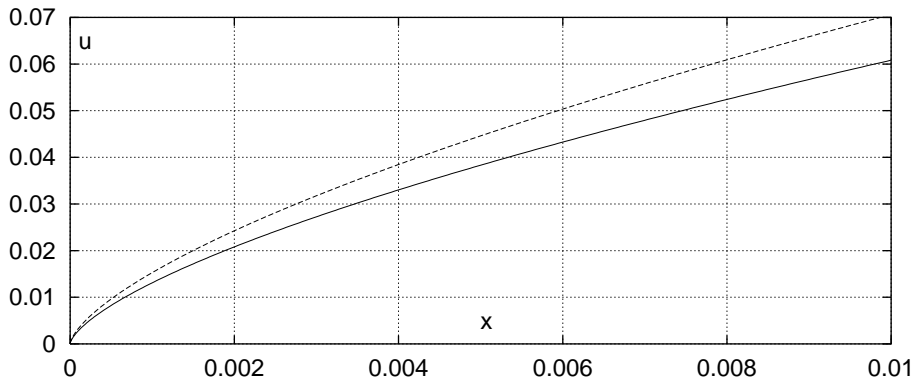


Figure 1: The profile at the moment of quenching for $\beta = 0.5$, $\gamma = 0.5$, $N = 1600$ - - - - computed; ———local analytical solution.

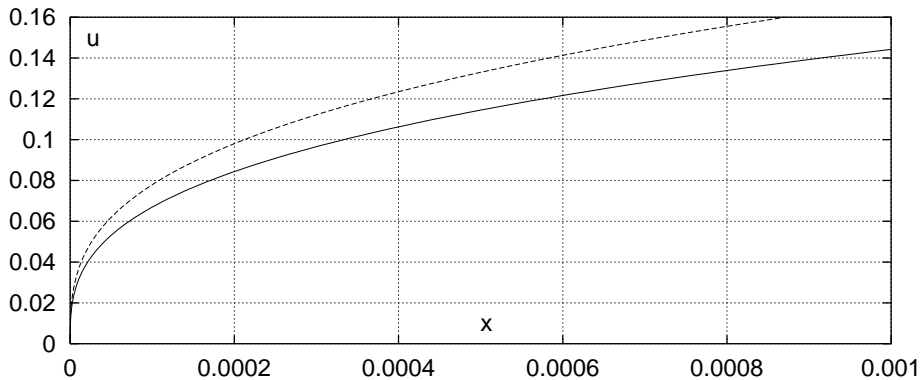


Figure 2: The profile at the moment of quenching for $\beta = 2$, $\gamma = 2$, $N = 1600$ - - - - computed; ———local analytical solution.

The agreement is quantitatively very good. Clearly no denser meshes are necessary due to the adequate choice for the non-uniform grid. In what follows the results are obtained with $N = 200$ unless it is specifically given another number in the text. It is also clearly seen that the asymptotic behavior of the calculated solution approaches the behavior of the singular local solution as $x \rightarrow 0$ which lends additional credibility to the results obtained here. Note the highly zoomed x -axis which exaggerates even the slightest differences between the different profiles.

The second case ($\beta = 0.5$, $\gamma = 2$) is rather similar to the first with the only difference that the temporal evolution is faster and this fact has to be accounted for in the initial selection of the time increment.

The third case ($\beta = 2$, $\gamma = 2$) is harder to treat numerically because of the higher-order of the singularity near $x = 0$ at the moment of quenching. Its temporal evolution is also faster than the one of first case. Once again we observed quenching for all different initial conditions we used. The result is presented in Fig. 2 for the region near the origin

of the coordinate system where the quenching takes place due to the nonlinear boundary condition. As already above mentioned the number of grid intervals is $N = 200$ and the x -axis is zoomed. Even with this small number of grid intervals we get accurate results because the non-uniform grid is dense in the vicinity of the origin and coarse in the regions where the changes of the sought functions are not moderate.

Next we treat the case (2.8) and we find no qualitative difference in the behavior in the sense that the quenching does occur and it happens at the boundary with the nonlinear boundary condition. The only quantitative difference is the time of quenching which depends on the initial condition. Hence, even when the third of the behavioral restrictions on the initial condition is not satisfied the quenching does take place.

Proceeding further we consider (2.9) when two of the behavioral conditions are not satisfied. The scenario is once again the same with some quantitative difference for the time of quenching. For the sake of diversity we consider this case for the $\beta = 0.5$ and $\gamma = 2$. In Figure 3 the obtained solution $u(x, t)$ is presented as a surface plot. One can judge about

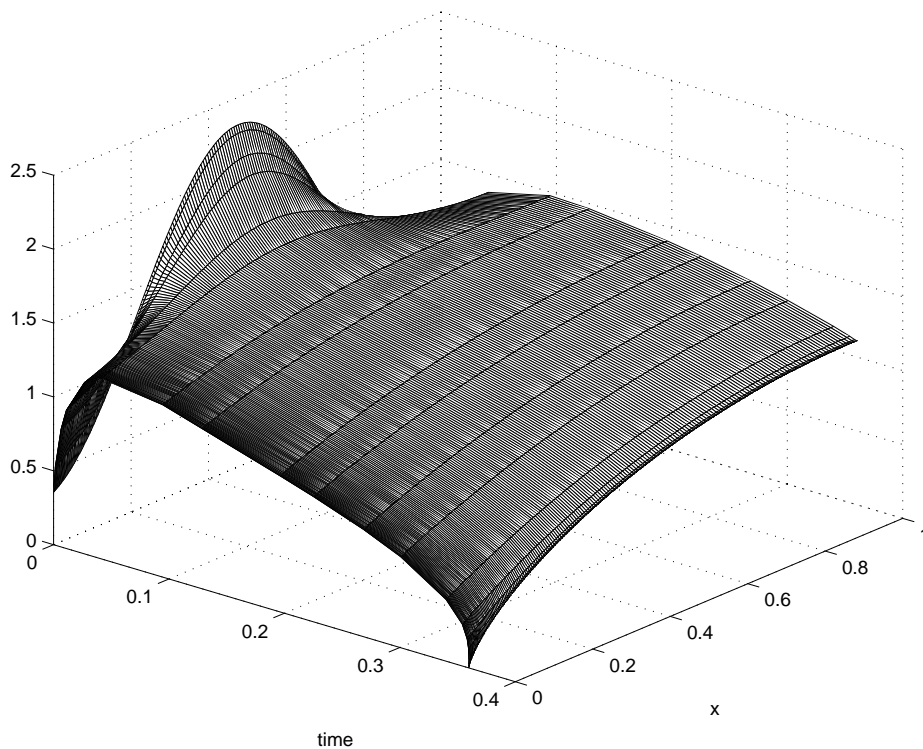


Figure 3: Surface plot of function $u(t, x)$ for $\beta = 0.5$ and $\gamma = 2$

the evolution of the time increment τ from the relative situation of the cross-sections parallel to the plane of the initial condition.

We observed a similar behavior also for the constant initial condition (2.10).

5.2 Quenching Rate (Theorem B)

As the quenching occurs for certain finite time $t = T$ the behavior of function u is supposed to obey the law

$$u(0, t)(T - t)^{-\frac{1}{\gamma+2\beta+1}} \rightarrow C \quad \text{for } t \rightarrow T, \quad (5.1)$$

or which is the same

$$u(0, t) \sim C(T - t)^{\frac{1}{\gamma+2\beta+1}}, \quad u_t(0, t) \sim -\frac{C}{\gamma + 2\beta + 1}(T - t)^{\frac{1}{\gamma+2\beta+1}-1}. \quad (5.2)$$

Notice that since $\mu = \frac{1}{\gamma+2\beta+1} < 1$, we have

$$u(0, t) \rightarrow 0, \quad u_t(0, t) \rightarrow -\infty \quad \text{for } t \rightarrow T. \quad (5.3)$$

The finite difference version of (5.2) reads

$$u(0, t^n) = \frac{1}{2}(u_{1,n} + u_{2,n}) + O(\tau^2),$$

where the superscript n refers to the current time stage. In our compilations we collect data for $u(0, t)$ and then recast it into different form which is shown in the figures to follow.

In all of the cases under consideration a quenching took place but the quenching time T depends on the actual shape of the initial condition. Hence a comparison which involves T explicitly does not make much sense. For this reason after the process of quenching is completed and the quenching time established we render $u(0, t)$ to $u(0, T - t)$ and present the results. In fact we extrapolate the quenching time T from the last two results for u , say u^N and u^{N-1} where N is the number of time step immediately before the last time stage (the stage at which the quenching takes place). Then

$$T = \frac{(t^N - t^{N-1}R)}{(1 - R)}, \quad R \stackrel{\text{def}}{=} \left(\frac{u^N}{u^{N-1}} \right)^{(\gamma+2\beta+1)}$$

For the case $\gamma = 0.5$ and $\beta = 0.5$ we present in Figure 4 the calculated $u(0, T - t)$ with three different resolutions. The best-fitting curve of type of (5.2) is juxtaposed to the numerical results. In this case the power in (5.2) is $(\gamma + 2\beta + 1)^{-1} = 0.4$.

As can be seen from the figure, the agreement for $u(0, t)$ between the calculations with different resolution is very good and the finest mesh gives a result which fits the result of Theorem B quantitatively very well. The deviations for the rougher mesh are inevitable due to the fact that the solution near the boundary becomes so small that it is submerged into the truncation error.

Qualitatively the same is the situation with all of the four cases considered here. Fig. 5 shows the results for the four cases with different dashed lines. The respective best-fit approximation is depicted with a solid line. It is clearly seen that in all of the cases the calculations confirm the expression for the behaviour of u as derived in Theorem B.

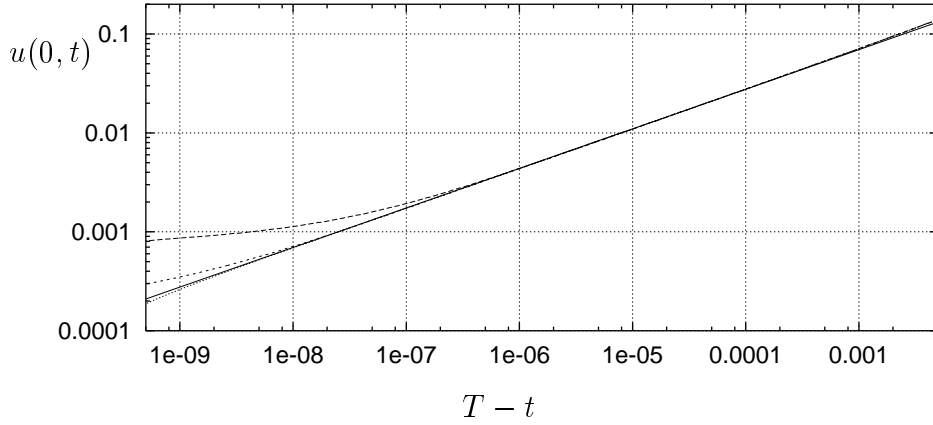


Figure 4: Quenching time for $\beta = 0.5$, $\gamma = 0.5$: - - - - - N=6400; - - - N=1600; - · - N=400; ——— $1.1(T - t)^{0.4}$.

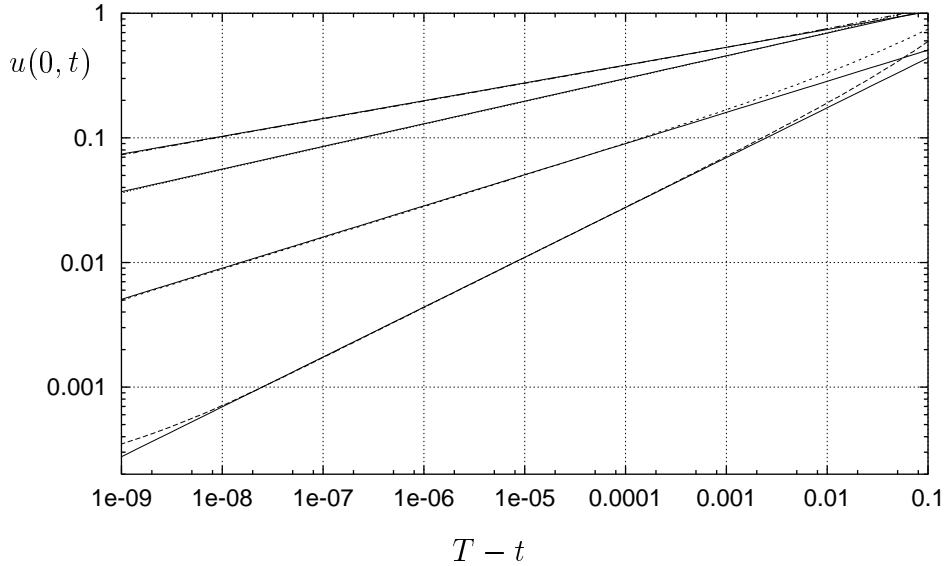


Figure 5: Quenching time for different sets of governing parameters: - · - $\beta = 2$, $\gamma = 2$ ($u(0, t) = 1.43(T - t)^{1/7}$); · · · · $\beta = 2$, $\gamma = 0.5$ ($u(0, t) = 1.6(T - t)^{1/5.5}$); - - - - $\beta = 0.5$, $\gamma = 2$ ($u(0, t) = 0.9(T - t)^{1/4}$); - · - $\beta = 0.5$, $\gamma = 0.5$ ($u(0, t) = 1.1(T - t)^{1/2.5}$).

6 Conclusions

The diffusion tends to smooth initial nonmonotone shapes. After they become reasonably close to the profiles which satisfy the conditions of Theorem A there begins a quick process of quenching.

For $\gamma \neq 1$ we have found numerically that all of the initial profiles inevitably lead to quenching. This is similar to the result of [4] for the linear diffusion equation $\gamma = 1$ under

nonlinear Neumann boundary condition. Hence one can consider our results as an extension of [4].

Acknowledgements

The work of CIC was supported through Grant No. R199524 by LaSPACE Consortium under LEGSF and NASA Grant NGT5-40035.

References

- [1] G. I. Barenblatt, Dynamics of turbulent spots and intrusions in stably stratified fluid, *Izvestiya Akademii Nauk SSSR, Fizika Atmosfery i Okeana*, **14** (1978), 195-206.
- [2] C. I. Christov and G. M. Homsy, Nonlinear dynamics of two-dimensional convection in a vertically stratified slot with and without gravity modulation, *J. Fluid Mechanics*, **430** (2001), 335-360.
- [3] K. Deng and M. Xu, Quenching for a nonlinear diffusion equation with a singular boundary condition, *Z. Angew. Math. Phys.*, **50** (1999), 574-584.
- [4] M. Fila and H. A. Levine, Quenching on the boundary, *Nonlinear Anal. TMA*, **21** (1993), 759-802.
- [5] H. A. Levine. The quenching of solutions of linear parabolic and hyperbolic equations with nonlinear boundary conditions, *SIAM J. Math. Anal.*, **14** (1983), 1139-1153.
- [6] P. R. Wallace, *Mathematical Analysis of Physical Problems*, (Dover, New York, 1984).